AIAA JOURNAL
Vol. 44, No. 11, November 2006

Self-Similarity in the Outer Region of Adverse-Pressure-Gradient Turbulent Boundary Layers

Yvan Maciel,* Karl-Stéphane Rossignol,† and Jean Lemay‡
Laval University, Quebec City, Quebec G1K 7P4, Canada

DOI: 10.2514/1.19234

This paper presents a consistent theory of self-similarity and of equilibrium in the outer region of turbulent boundary layers that explains recent experimental findings on the subject, including new ones presented here. The theory is first presented in a general form where the outer scales are left unspecified and it is not assumed that the mean velocity defect and the Reynolds stresses share a common velocity scale. It is shown that the main results of the traditional similarity theory remain valid even in this case. Common outer scaling with the Zagarola–Smits length and velocity scales is then chosen. A new pressure gradient parameter is introduced to characterize the local effect of the pressure gradient in all flow conditions including strong adverse-pressure-gradient conditions. By analyzing several adverse-pressure-gradient flow cases, it is shown that self-similarity of the mean velocity defect profile is reached in all cases in localized but significant flow regions. The same is, however, not true of the Reynolds stress profiles. In agreement with the similarity analysis, the self-similar velocity defect profile is found to be a function of the pressure gradient and most flows studied here are only in an approximate state of equilibrium in the region of self-similar defect profiles despite the excellent collapse of the profiles.

Nomenclature

C_f = skin friction coefficient, $2\tau_w/\rho U_e^2$
G = defect shape factor
H = shape factor, δ^*/θ
L_e = external flow length scale
L_i = inner-region length scale
L_o = outer-region length scale
p_e = freestream static pressure
Re = local Reynolds number, $U_e L_o/\nu$
Re_θ = momentum-thickness Reynolds number, $U_e\theta/\nu$
T_e = external flow time scale
T_o = outer-region time scale
U, V = streamwise and wall-normal mean velocity components
U_{ZS} = Zagarola–Smits velocity, $U_e\delta^*/\delta$
U_e = freestream velocity
U_o = outer-region velocity scale
u_τ = skin friction velocity, $(\tau_w/\rho)^{1/2}$
x = streamwise coordinate
x_{min} = position x of the first measurement station of a data set
x_{max} = position x of the last measurement station of a data set
x_o = virtual origin of the equilibrium state
y = wall-normal coordinate
β = pressure gradient parameter, $-(L_o/U_o)\,\mathrm{d}U_e/\mathrm{d}x$
β_T = Clauser's or Rotta–Clauser's pressure gradient parameter, $-(\Delta/u_\tau)\,\mathrm{d}U_e/\mathrm{d}x$
β_{ZS} = pressure gradient parameter with ZS scaling, $-(\delta/U_{ZS})\,\mathrm{d}U_e/\mathrm{d}x$
γ = velocity ratio U_o/U_e
γ_T = velocity ratio with traditional scaling u_τ/U_e
γ_{ZS} = velocity ratio with ZS scaling U_{ZS}/U_e
Δ = Rotta–Clauser length scale, $\delta^* U_e/u_\tau$
Δx = streamwise extent of the self-similar zone
δ = boundary layer thickness
δ_{av} = average boundary layer thickness over a given number of measurement stations
δ_{99} = δ corresponding to $U = 0.99U_e$
δ^* = displacement thickness
η = y/L_o
θ = momentum thickness
Λ = similarity parameter, $-(L_o\,\mathrm{d}U_e/\mathrm{d}x)/(U_e\,\mathrm{d}L_o/\mathrm{d}x)$
ν = kinematic viscosity
Π = pressure gradient parameter, β/γ
ρ = density
τ_w = skin friction

Subscripts

e = external flow at outer edge of boundary layer
T = traditional scaling with Δ and u_τ
ZS = Zagarola–Smits scaling with δ and U_{ZS}

Received 30 July 2005; revision received 10 April 2006; accepted for publication 11 April 2006.

*Professor, Department of Mechanical Engineering; ymaciel@gmc.ulaval.ca. Member AIAA.
†M.Sc. Student, Department of Mechanical Engineering. Student Member AIAA.
‡Professor, Department of Mechanical Engineering. Member AIAA.

I. Introduction

OVER the past decade, many new ideas have come to challenge the traditional theory of turbulent wall flows (see Buschmann and Gad-el-Hak [1], George [2], and Panton [3] for recent reviews). Some address the important and related issues of the choice of the appropriate length and velocity scales in the outer region of turbulent wall flows and of equilibrium in the outer region of turbulent boundary layers (TBL). This paper attempts to put into perspective the impact of recent findings dealing with these two issues in the case of 2-D TBL and more specifically in the case of adverse-pressure-gradient TBL.

To avoid any confusion, it is important to define beforehand the concepts of flow equilibrium and self-similarity and their connection. In this paper and in all the similarity theories that will be discussed, flow equilibrium means that all the terms in the governing equations must maintain the same relative weight as the flow develops. Thus, the properties of an equilibrium flow can evolve in the streamwise direction but the flow remains dynamically similar. The concept of self-similarity of turbulent flows, also called self-preservation or local similarity, is closely related to the concept of equilibrium. A turbulent flow is self-similar if its statistical properties, or at least some of them, depend only on local flow variables (scales). If a turbulent flow reaches a self-similar state, then

it can depend only on its upstream history through its length and velocity scales. It has therefore become an equilibrium flow.

A typical example of self-similar flows is the far field of turbulent free shear layers such as jets and wakes. In the context of 2-D TBL, self-similarity in the outer region is traditionally assumed to exist in the following form:

$$\begin{aligned} \frac{U_e - U}{u_\tau} &= \dot{f}(y/\Delta), & \frac{-\overline{u'v'}}{u_\tau^2} &= g_{12}(y/\Delta) \\ \frac{\overline{u'^2}}{u_\tau^2} &= g_{11}(y/\Delta), & \frac{\overline{v'^2}}{u_\tau^2} &= g_{22}(y/\Delta) \end{aligned} \tag{1}$$

The dot on f denotes differentiation with respect to y/Δ. These self-similar relations imply that the mean velocity defect and Reynolds stresses share common length and velocity scales, the Rotta–Clauser length scale Δ and the friction velocity u_τ. The boundary layer thickness δ is sometimes used instead of Δ as the length scale. Both scales are valid. The boundary layers corresponding to relations (1), first studied experimentally by Clauser [4] and first treated theoretically by Rotta [5,6] and Townsend [7,8], are traditionally called "equilibrium boundary layers." This expression will not be used here because of the nuance in meaning between the terms equilibrium and self-similarity we wish to emphasize.

As such, flow equilibrium does not imply and is not restricted to any particular type of self-similarity of some statistical properties of the flow. Different similarity analyses basically start with different assumptions on the type of self-similarity that should be encountered. They differ primarily on the type of scaling used. But they all imply flow equilibrium. They therefore lead to different similarity conditions, some more restrictive than others, which characterize particular classes of equilibrium flows. In other words, a flow (or flow region) can be in equilibrium even if a particular similarity theory does not apply. Conversely, if a flow is found to be in equilibrium according to a given similarity analysis then it is in equilibrium regardless of the similarity assumptions.

Thus, the self-similar boundary layers mentioned previously are indeed in equilibrium in their outer region but these equilibrium conditions are not the only ones possible. We will refer to this important class of self-similar boundary layers as the "traditional equilibrium" boundary layers. In practice, these self-similar TBLs are rather the exception than the rule. There are only a few experimental realizations [4,9–12], with varying degrees of success, of the traditional equilibrium TBL in nonzero pressure gradient conditions.

Castillo and George [13] (herein denoted CG) have recently reconsidered the question of self-similarity and flow equilibrium in the outer part of TBL. They used a different similarity analysis to astonishingly conclude that most TBLs, whatever the pressure distribution, can be considered to be in a state of equilibrium, contrary to the traditional belief. In their analysis, CG assumed the following self-similar relations in the limit of an infinite local Reynolds number:

$$\begin{aligned} \frac{U_e - U}{U_o} &= \dot{f}(y/\delta), & \frac{-\overline{u'v'}}{R_{12}} &= g_{12}(y/\delta) \\ \frac{\overline{u'^2}}{R_{11}} &= g_{11}(y/\delta), & \frac{\overline{v'^2}}{R_{22}} &= g_{22}(y/\delta) \end{aligned} \tag{2}$$

According to them, the only condition necessary for self-similarity of type (2) is

$$\Lambda = \frac{\delta}{\mathrm{d}\delta/\mathrm{d}x}\frac{\mathrm{d}p_e/\mathrm{d}x}{\rho U_e^2} = -\frac{\delta}{\mathrm{d}\delta/\mathrm{d}x}\frac{\mathrm{d}U_e/\mathrm{d}x}{U_e} = \text{const} \tag{3}$$

The analysis led also to the following conditions, which they treated as outer scale definitions:

$$\gamma = \frac{U_o}{U_e} = \text{const} \tag{4}$$

$$\frac{R_{12}}{U_e^2(\mathrm{d}\delta/\mathrm{d}x)} = \text{const} \tag{5}$$

$$\frac{R_{11}}{U_e^2} = \text{const} \tag{6}$$

$$\frac{R_{22}}{U_e^2} = \text{const} \tag{7}$$

They therefore considered that the outer scales for the velocity defect, Reynolds normal stresses and Reynolds shear stress are, respectively, U_e, U_e^2, and $U_e^2\,\mathrm{d}\delta/\mathrm{d}x$.

CG used six adverse-pressure-gradient (APG), three favorable-pressure-gradient (FPG), and one zero-pressure-gradient (ZPG) experimental databases to show that turbulent boundary layers appear to be characterized by only three possible values of Λ within experimental uncertainty (0.22 for APG, 0 for ZPG, and -1.92 for FPG). They concluded from this observation that almost all pressure gradient (PG) TBLs, including very strong APG cases, appear to be equilibrium boundary layers since Eq. (3) is satisfied. CG further argued that the data can indeed be collapsed into only three velocity defect profiles, but only when the outer velocity scale U_{ZS} proposed by Zagarola and Smits [14] (discussed later) is used instead of U_e. By assuming that δ^*/δ tends to a nonzero constant when $Re_\theta \to \infty$, they argued that these two velocity scales are equivalent in the limit of an infinite Re_θ and are therefore both consistent with their similarity analysis. Note that in the commonly accepted view of the asymptotic behavior of TBL, $\delta^*/\delta \to 0$ as $Re_\theta \to \infty$ and U_{ZS} therefore becomes equivalent to u_τ in that limit and not U_e.

Castillo et al. [15] found that TBLs for which Λ is constant tend to maintain Λ constant as they approach separation. Castillo and Wang [16] used four experimental databases of nonequilibrium boundary layers (Λ varies) to show that even nonequilibrium flows, such as those over airfoils or with sudden changes of pressure gradient, go rapidly from one constant value of Λ (the FPG, ZPG, or APG one) to another. Following the same reasoning as CG, Castillo et al. [15] and Castillo and Wang [16] concluded that these dominant regions of constant Λ correspond to regions of equilibrium flow. Furthermore, for all the nonequilibrium flows, Castillo and Wang found that the velocity defect profiles in the constant Λ zones collapse with those of "APG equilibrium boundary layers" (meaning APG TBL for which Λ is constant) when scaled with U_{ZS}.

Castillo, George, and coworkers' conclusions that flow equilibrium is found in almost all PG conditions and that there can be only three possible limiting velocity profiles (one each for ZPG, APG, and FPG boundary layers) are astonishing ones. They rest on the assumption that condition (3) is a necessary and sufficient condition for complete self-similarity. It will be shown in this paper that experiments do not confirm these conclusions and moreover that they cannot be inferred from the similarity differential equation obtained by CG. By analyzing the similarity equation in the light of experimental results, opposite conclusions will be found, namely, that universal self-similar profiles (one each for ZPG, APG, and FPG boundary layers) do not exist and that TBLs found in the real world are almost never in a state of equilibrium, although they tend to approach it in some cases.

The work of Castillo and coworkers has revealed the interesting potential of U_{ZS} as an outer velocity scale. Traditionally, u_τ is used as the turbulent velocity scale and hence the outer velocity scale for boundary layers. This choice has often been questioned by many researchers but the debate has intensified over the last few years because of the recent developments in boundary layer theory and the availability of modern high-quality experiments. A recent review over this debate which points out the essential differences between the various velocity scales proposed can be found in Panton [3].

Because we wish to consider in this paper PG flows in general including cases very close to separation, u_τ is definitely not an appropriate turbulent or outer velocity scale. As was mentioned previously, CG have proposed U_e as the outer velocity scale. Panton [3] discards the use of U_e based on the fact that it is not a turbulent

velocity scale because it does not scale with the Reynolds shear stress. The velocity defect profile is in part the result of the Reynolds shear stress. Panton therefore claims that using U_e as the outer velocity scale is logically inconsistent because the velocity defect formulation becomes then independent of the Reynolds shear stress.

One very important and practical type of flow suffices to show that U_e^2 and $U_e^2\,\mathrm{d}\delta/\mathrm{d}x$ are not outer scales for the Reynolds stresses. It is the flow on the suction side of an airfoil at high angle of attack which goes from strong FPG to strong APG. In such a flow, the Reynolds stresses scaled with U_e^2 can grow by 1 order of magnitude in the outer region of the TBL. Note that u_τ^2 is an even worst scaling variable because the change of magnitude can be even infinite in such a flow.

Zagarola and Smits [14] have proposed $U_c - U_b$ as the outer velocity scale for turbulent pipe flow, where U_c is the centerline velocity and U_b is the bulk mean velocity. They showed that $U_c - U_b$ was better than u_τ in collapsing the velocity defect profiles. They further proposed an equivalent scale for the TBL, namely, $U_{ZS} = U_e\delta^*/\delta$. These two scales are basically proportional to the deficit of mass flow rate due to the presence of a wall. As mentioned previously, CG, Castillo et al. [15], and Castillo and Wang [16] showed that U_{ZS} is successful in collapsing, at least to some extent, the defect profiles for almost all the APG, FPG, ZPG, and complex PG flow cases they studied. Based on the similarity analysis of CG and on a separation of variables assumption, Castillo and Walker [17] argued that the scale U_{ZS} removes the effects of both the upstream conditions and finite local Reynolds number on the velocity defect profiles. By a completely different approach, namely, composite expansions, Panton [3] showed that scaling with U_{ZS} is equivalent to using a higher order theory. The ZS scaling therefore automatically reduces the level of dependency on Reynolds number and upstream conditions of the scaling laws, but not completely.

Maciel et al. (MRL) [18] have recently shown that U_{ZS}^2 scales all the Reynolds stresses in the outer region of an APG TBL where the TBL was subjected to a very strong APG leading to separation and had experienced an abrupt transition from strong FPG to strong APG. In that flow, U_e^2 and u_τ^2 were definitely not outer scales for the Reynolds stresses. Buschmann and Gad-el-Hak [19] have found that even in the inner region of ZPG TBL, channel and pipe flows, the ZS scaling is as good as the classical scaling based on u_τ. The velocity scale U_{ZS} appears therefore more "universal" than u_τ in the sense that it can be used in both regions of turbulent wall flows and for all flow conditions (FPG, ZPG, APG, complex PG, rough wall, ...). Let us note that Mellor and Gibson [20] and Perry and Schofield [21] have proposed pairs of length and velocity scales specifically developed for the outer region of APG TBL. But these scales are cumbersome to use; they lack of generality and from experience we find that they do not reveal in general self-similarity like U_{ZS} and δ do.

To obtain flow equilibrium, self-similarity of the Reynolds stresses is also required. For APG TBL corresponding to the traditional definition of equilibrium boundary layers, the experiment of Skåre and Krogstad (SK) [12] showed self-similarity of the Reynolds stresses and triple correlations with either u_τ or U_e as an outer velocity scale. For APG boundary layers which do not correspond to traditional equilibrium boundary layers, self-similarity of the Reynolds stresses is seldom found and usually not with the same scales as the mean flow. In an experimental study of a boundary layer that is maintained on the verge of separation, Dengel and Fernholz (DF) [22] obtained self-similar velocity defect profiles with the Perry–Schofield scalings but only in the vicinity of separation. They did not find similarity for the turbulent quantities. In a similar study, Elsberry et al. [23] found different length and velocity scales for mean velocity and for the various Reynolds stresses, which led them to conclude that the flow exhibited a lack of equilibrium. In a separation bubble experiment at high Reynolds number, Angele [24] found some degree of self-similarity of the turbulence quantities with both the Mellor–Gibson and Perry–Schofield scalings although far from complete.

Self-similarity of the Reynolds stresses with the same outer length and velocity scales as the mean flow (the ZS scales) has only been reported once [18]. Surprisingly, this complete self-similarity with common scales occurred near separation for a flow where the boundary layer was subjected to a very strong APG and had experienced an abrupt transition from strong favorable to strong adverse pressure gradients.

This paper revisits the issues of self-similarity, equilibrium, and scaling in the outer region of TBL. The main objectives are to put into perspective the impact of recent findings on the subject, including new results presented here, and to provide a consistent theory to explain them. We start by examining the profiles of six APG high-quality experimental databases to establish the extent of self-similarity of the velocity defect and Reynolds stress profiles that is obtained with the ZS scaling. To explain the surprising extent and type (complete or incomplete) of self-similarity observed here and in the aforementioned studies, a similarity analysis of the outer region of TBL is then presented in a general form that encompasses all the various similarity analyses found in the literature. Divergent theories and their implications are discussed. Empirical evidence and theoretical arguments are given to support the theory based on the classical treatment of turbulence. In the process, we provide a clear interpretation of the similarity equations, conditions, and parameters. The theory is then used to understand the empirically observed self-similarity. The degree of equilibrium (corresponding to complete self-similarity with the ZS scaling) of the various flows studied here is assessed by looking at the evolution of the similarity parameters.

II. Observed Self-Similarity

In this section, velocity defect and Reynolds stress profiles of six APG high-quality experimental databases are examined to determine to what extent self-similarity is revealed by the ZS scaling. All the profiles presented are therefore scaled with U_{ZS} and δ (here δ is always δ_{99}). Table 1 presents the six databases used and for each flow case, the corresponding ranges of the boundary layer parameters. The flow cases are listed in approximate order of increasing severity of the pressure gradient distribution imposed on the boundary layer. The ordering was not done with Clauser's pressure gradient parameter β_T but with a new pressure gradient parameter that will be presented in the next section. The severity of the pressure gradient distribution can, however, be approximately guessed by the values of H, C_f, and β_T at the last station of each flow (generally the values on the right of each range expression).

Flows SJ (Samuel and Joubert), MP10, and MP30 (Marusic and Perry) correspond to mild APG cases where the pressure gradient increases and then decreases. Flow SK, which was already discussed

Table 1 APG TBL databases used and the corresponding ranges of the boundary layer parameters

Experiment	Re_θ	H	$C_f \times 10^3$	β_T
Samuel and Joubert [25] (SJ)	——	1.39–1.61	2.76–1.25	0.0756–8.023
Marusic and Perry [26] 30APG (MP30)	6430–19,100	1.40–1.60	2.87–1.38	0–6.07
Marusic and Perry 10APG (MP10)	2200–7260	1.43–1.73	3.6–1.37	1–7.16
Skåre and Krogstad (SK) [15]	39,100–54,000	2.01–1.99	0.59–0.54	19.6–21.4
Perry [27] (P)	15,900–97,200	1.42–2.41	1.98–0.24	2.35–71.2
Dengel and Fernholz [22] case 2 (DF2)	1260–9600	1.46–2.53	3.59–0.12	$\sim$0–∞
Dengel and Fernholz case 1 (DF1)	1300–10,000	1.46–2.83	3.51–(−0.02)	$\sim$0–∞
Dengel and Fernholz case 3 (DF3)	1300–11,200	1.46–3.21	3.52–(−0.16)	$\sim$0–∞
Maciel et al. (MRL) [18]	3360–14,300	1.72–4.11	18.7–(−0.08)	320–∞

in the Introduction, is a very good approximation of a traditional equilibrium TBL ($\beta_T \approx$ const, $C_f \approx$ const). As can be seen in Table 1, the variations of C_f and β_T are relatively small for this flow. Flow *P* is a strong APG case of decreasing pressure gradient where separation of the boundary layer downstream of the measurement stations was avoided by a contraction at the end of the test section. The DF flows are three flow cases of boundary layers in the vicinity of separation with only slightly different pressure distributions (increasing PG followed by decreasing PG). They are characterized by different values of the minimum skin friction: case 1, approximately zero; case 2, slightly positive; and case 3, slightly negative (long, shallow separation bubble). Flow MRL corresponds to an APG TBL similar to those found on the suction side of airfoils in trailing-edge post-stall conditions. The TBL has suffered from an abrupt transition from very strong FPG to very strong APG, leading to a nonreattaching large separation zone. The measurements were made only in the APG zone, that is, downstream of the pressure peak where the PG is progressively decreasing, with one station at the detachment position.

Flow MRL is used first to illustrate a typical streamwise evolution of the velocity defect profile. Five velocity defect profiles scaled with ZS of the MRL flow are presented in Fig. 1. The streamwise positions are expressed with the normalized variable $(x - x_{\min})/\delta_{\text{av}}$ to appreciate the distance between the positions with respect to the outer length scale. The variable $x_{\min}$ corresponds to the position of the first measurement station and δ_{av} is the average of the boundary layer thicknesses of the five stations shown. The monotonous evolution shown in Fig. 1 is representative of the transition from an FPG or ZPG behavior to an APG one. The first profile is at the start of the APG zone and it is actually very close to the FPG self-similar profiles shown by CG. All the other flows evolve qualitatively in the same manner as flow MRL except SJ. In the latter flow, a similar evolution occurs at the beginning, followed by self-similarity of the profiles of stations 3–10, but then the last two stations (11 and 12) show a slight increase in the velocity deficit.

Returning to Fig. 1, we can see that the last two profiles collapse extremely well. Note that the last station shown is at the location of detachment, that is, $C_f = 0$. Plots such as those of Fig. 1 are used to find self-similarity. Profiles are considered self-similar only if the collapse is found to be excellent. Figure 2 shows the self-similar velocity profiles for all flows. In all cases, self-similarity can indeed be found and it is not fortuitous. The three flow cases of DF have been combined because they cannot be distinguished. The same is true for the two flow cases of MP.

To be meaningful, self-similarity has to exist over a reasonably long streamwise distance. The streamwise extent of the zones where collapse of the velocity defect profiles has been found, Δx, is shown in Fig. 2 as a function of the average boundary layer thickness in these zones, δ_{av} (δ_{av} for MRL is therefore different than the δ_{av} used in Fig. 1 which was the average over all stations). In all flow cases, it is seen that Δx exceeds or equals $2\delta_{\text{av}}$. For these APG flows, especially the strong APG ones, the mean flow and Reynolds stress profiles evolve considerably over a distance of $2\delta_{\text{av}}$. For instance, for the MRL flow, both the boundary layer thickness and the maximum turbulence intensity increase by about 33% between the two positions shown in Fig. 2. Even in the two much milder APG flow cases of MP, the boundary layer thickness increases by about 15% and the maximum turbulence intensity increases by 35% between the two measurement stations where collapse of the velocity defect profiles was found. The nine flow cases presented in Fig. 2 therefore all exhibit local but significant zones of self-similarity of the velocity defect profiles when ZS scaling is used.

Table 2 summarizes the information on the profiles that are self-similar, including the range of values of the traditional similarity parameters γ_T and β_T. The traditional similarity parameters are clearly not constant, except of course for the SK flow, in the self-similar flow zones revealed by the ZS scaling. Thus, the self-similarity zones of all these flows, except the SK one, are far from being equilibrium flow zones in the traditional sense.

In all flow cases, the parameter Λ was found to be approximately constant. Recall that this corresponds to one of the conditions of

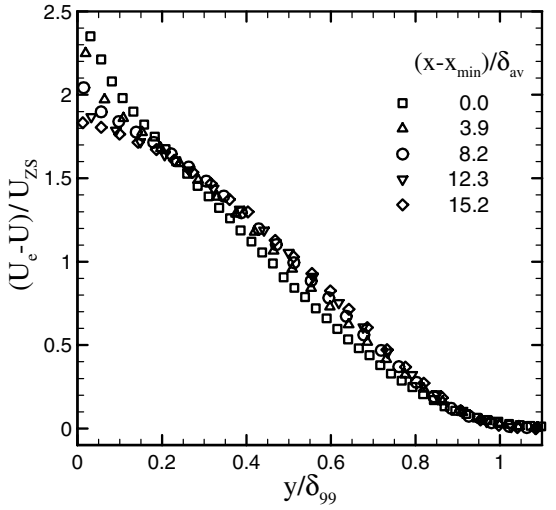

Fig. 1 Velocity defect profiles of MRL scaled with U_{ZS} and δ (here $\delta = \delta_{99}$). Five profiles up to detachment.

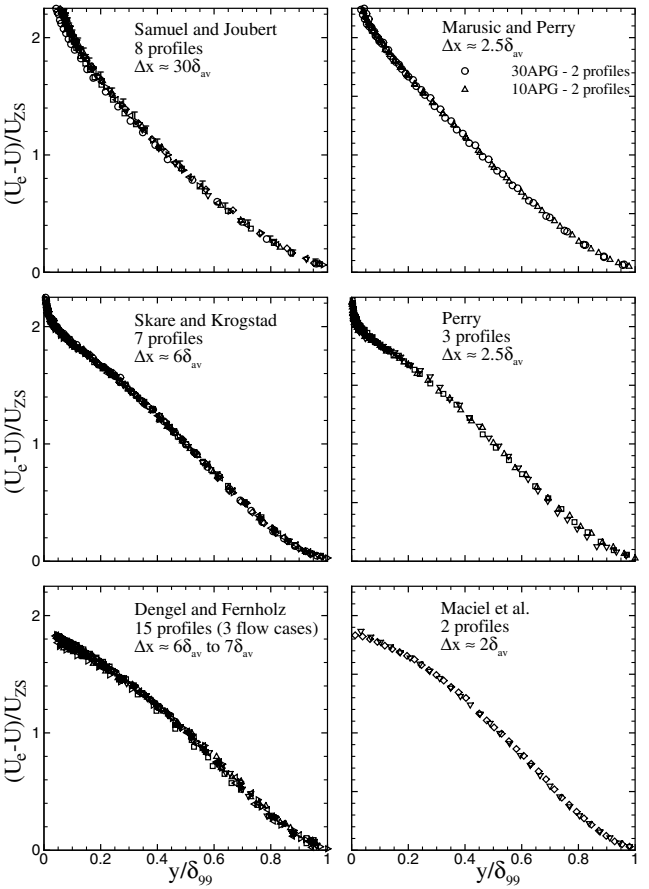

Fig. 2 Self-similar velocity defect profiles scaled with U_{ZS} and δ (here $\delta = \delta_{99}$). For each flow case, Δx is the streamwise distance covered by the profiles shown, and δ_{av} is the average boundary layer thickness for the range of profiles shown.

CG's similarity analysis, Eq. (3), and actually of the traditional similarity analysis also (see next section). The values of Λ are similar but not identical for these APG flows, and no clear trend with PG conditions is revealed. A further discussion of the parameter Λ will be presented in the next two sections.

The shape of the self-similar profiles shown in Fig. 2 definitely depends on the severity of the pressure gradient distribution imposed on the boundary layer. To better illustrate this point, Fig. 3 combines the self-similar profiles of MP, SK, DF, and MRL in a close-up view.

Table 2 Self-similar stations and the corresponding boundary layer parameters

Experiment	Stations showing self-similarity with ZS	Self-similarity of Reynolds stresses	Re_θ	H	$C_f \times 10^3$	Λ	$\gamma_T \times 10^2$	β_T
SJ	3–10 out of 12	No	——	1.39–1.48	2.60–1.88	0.22	3.61–3.07	0.230–2.91
MP30	Last 2 out of 6	No	16,600–19,100	1.54–1.60	1.62–1.38	0.33	2.84–2.63	3.96–6.07
MP10	Last 2 out of 6	No	6360–7260	1.64–1.73	1.68–1.37	0.30	2.90–2.62	4.48–7.16
SK	All 7 stations	Yes	39,120–53,970	2.01–1.99	0.59–0.54	0.22	1.72–1.64	19.9–21.4
P	Last 3 out of 10	No data	79,600–97,200	2.01–1.99	0.48–0.24	0.16	1.55–1.09	28.0–71.2
DF2	7 to 11 out of 12	?	4600–8700	2.21–2.53	0.35–0.12	0.19	1.32–0.78	41,000–170000
DF1	7 to 11 out of 12	?	5200–10,000	2.31–2.83	0.25–(−0.02)	0.20	1.11–0	59,000–∞
DF3	7 to 11 out of 12	?	5700–9300	2.47–3.05	0.13–(−0.16)	0.17	0.81–0	120,000–∞
MRL	4 and 5 out of 6	Yes	11,000–12,700	3.09–3.85	0.159–0	0.18	0.89–0	72,000–∞

The differences in shape are obvious. Castillo and coworkers' assertion [13,15–17] that there can be only one possible limiting velocity profile for APG TBL is clearly not confirmed by the data. The effect of upstream conditions, essentially the pressure gradient effects in the cases studied, will always be reflected in the self-similar profiles. This will be seen even more clearly with the Reynolds stress profiles. It should be noted also, as it will be shown in the next section, that the area under the curve of the velocity defect plots scaled with ZS is necessarily one. Therefore, the defect profiles of two totally different flows can only differ by their shape when plotted with the ZS scaling. This implies that they can easily exhibit an apparent similarity if they are plotted with wide axis ranges.

Figures 4 and 5 present the Reynolds stress profiles scaled with ZS at the stations that were considered self-similar based on the velocity defect profiles (see Table 2). The flow cases with milder APG are shown in Fig. 4 and the ones with stronger APG in Fig. 5. Reynolds stress data are available for all flow cases except flow *P*. No data for $\overline{v'^2}$ are shown for the DF flow cases because the authors indicate that the pulsed-wire uncertainties are too high for that Reynolds stress. Pulsed-wire uncertainties are, however, also fairly high for $\overline{u'^2}$ and $\overline{u'v'}$ (8 and 20%, respectively, according to DF). The profiles for flow case 3 seem to have even higher uncertainties and are therefore not presented.

The Reynolds stress profiles of the mild APG cases presented in Fig. 4 do not show self-similarity. For the strong APG flow cases, Fig. 5, it is more difficult to draw definite conclusions on the degree of self-similarity of the Reynolds stress profiles due to the high uncertainties of the Reynolds stresses. Self-similarity is not apparent for the SK and DF profiles except maybe in the case of the Reynolds shear stress profiles of SK. However, self-similarity of all Reynolds stresses can be found in shorter streamwise distances for the SK flow. A close look at the data reveals that the Reynolds stress profiles at $x = 4.0$, 4.2, and 4.4 m collapse well together whereas the ones at $x = 4.6$ and 5.0 m also collapse well together. This corresponds to a

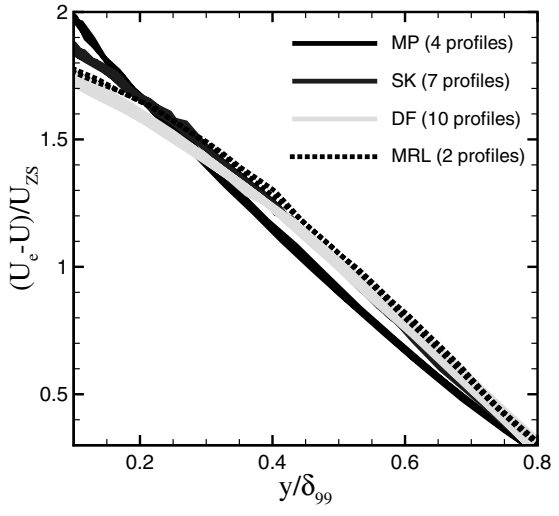

Fig. 3 Close-up view of the self-similar profiles for four flow cases.

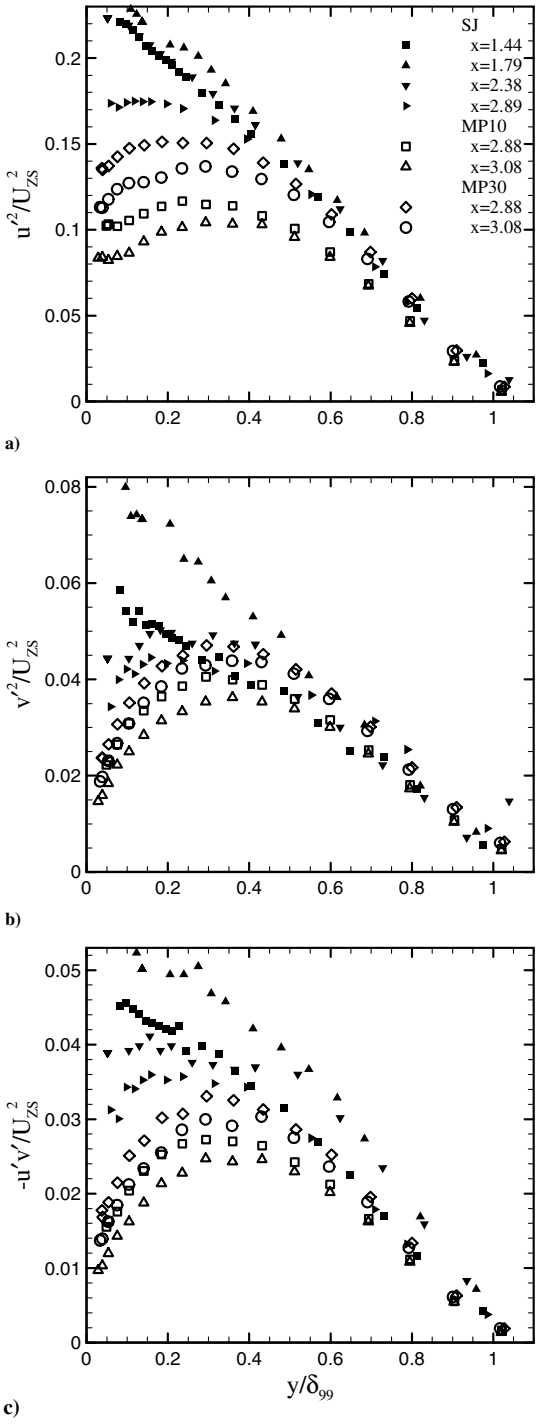

Fig. 4 Reynolds stress profiles of SJ and MP corresponding to positions of self-similar defect profiles.

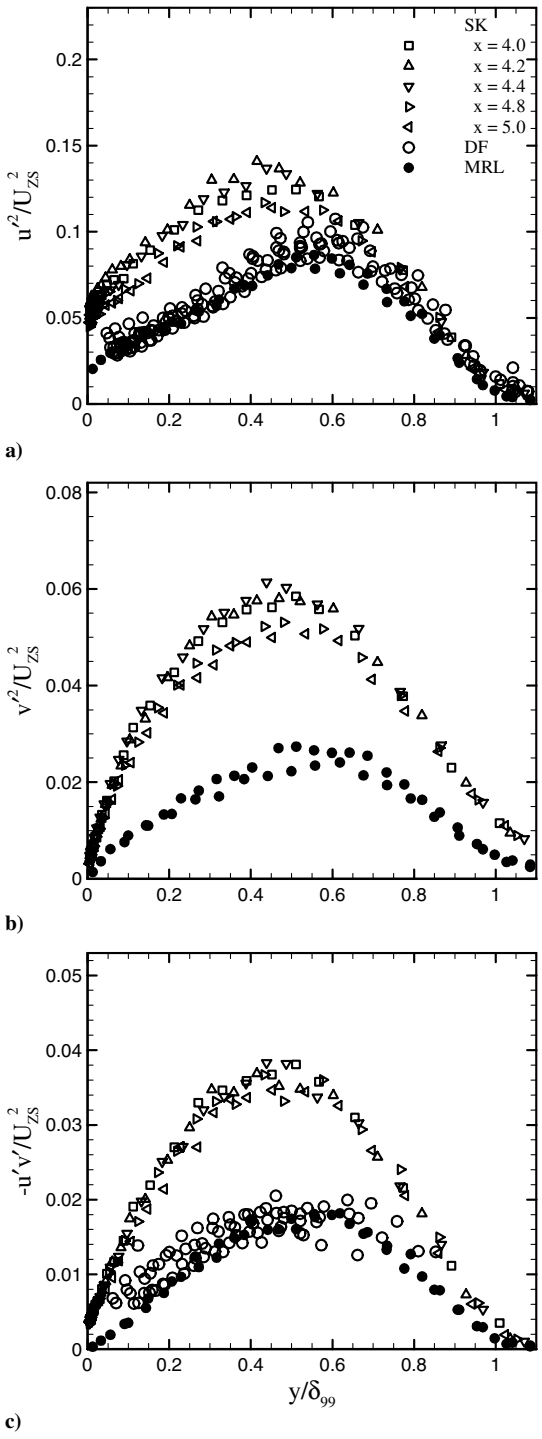

Fig. 5 Reynolds stress profiles of SK, DF, and MRL corresponding to positions of self-similar defect profiles.

collapse over a streamwise distance of roughly 2δ, which is still significant.

Turning our attention to the MRL flow now, the collapse of the Reynolds stress profiles presented in Fig. 5 is quite remarkable, especially if one keeps in mind the rapid streamwise evolution of the PG conditions and of the boundary layer characteristics of this flow. As was mentioned before, both the boundary layer thickness and the maximum turbulence intensity increase by about 33% between the two positions of self-similarity of the MRL flow shown in Fig. 5. In an attempt to explain why equilibrium or near equilibrium surprisingly seems to exist in this flow in the region just before detachment, MRL have noted that the two advection terms of the streamwise-mean-momentum equation dominate all the other terms (the stress gradient terms) in the outer region and almost balance themselves. In other words, the pressure force and the turbulent transport no longer play an important dynamic role close to separation. The outer region of the TBL has therefore become essentially an inertial flow zone where equilibrium is likely to occur.

As expected, the various Reynolds stress profiles presented in Figs. 4 and 5 show that the location of the maximum of the Reynolds stresses is a function of the PG strength. This will always be the case whatever the choice of outer velocity scale and it can only be changed by using a different length scale. Because the shape of the profiles varies also with the PG strength, it is pointless to look for universal self-similar profiles for the Reynolds stresses. Note, however, that the DF and MRL Reynolds stress profiles are surprisingly very much alike although the PG conditions are not the same.

III. Similarity Analysis

A. General Theory

We now seek a new theoretical framework that would help to understand the surprising extent of self-similarity obtained with the ZS scaling because as it will be shown in this section it cannot be explained with the traditional or CG's similarity analysis. We have, however, decided to use a "classical" similarity analysis analogous in many respects to the traditional ones [5–8,20] and the one done by CG because it was found to be adequate. The similarity analysis of the outer region of TBL will be presented in a general form that encompasses all the various similarity analyses found in the literature. A two-region structure of the TBL, namely, inner and outer regions, will be assumed at some places but the theory is not necessarily restricted to it.

The continuity and momentum equations for the outer region of incompressible and two-dimensional TBL are

$$\frac{\partial U}{\partial x} + \frac{\partial V}{\partial y} = 0 \tag{8}$$

$$U\frac{\partial U}{\partial x} + V\frac{\partial U}{\partial y} = U_e\frac{\mathrm{d}U_e}{\mathrm{d}x} - \frac{\partial \overline{u'v'}}{\partial y} + \frac{\partial}{\partial x}(\overline{v'^2} - \overline{u'^2}) \tag{9}$$

The viscous term has been neglected. The Reynolds normal stress terms have been kept because they are not necessarily negligible close to separation. The similarity analysis is first written in a general form in which the outer scales L_o, U_o, R_{12}, R_{11}, and R_{22} are left unspecified. We are looking for self-similarity of the form

$$\frac{U_e - U}{U_o} = \dot{f}(\eta) \tag{10}$$

$$\frac{-\overline{u'v'}}{R_{12}} = g_{12}(\eta), \qquad \frac{\overline{u'^2}}{R_{11}} = g_{11}(\eta), \qquad \frac{\overline{v'^2}}{R_{22}} = g_{22}(\eta) \tag{11}$$

The dot on f denotes differentiation with respect to $\eta = y/L_o$. Note that it is required only that these relations be valid in the outer region of the boundary layer. From a mathematical perspective, it will be more convenient to define the domain of validity as $\eta_L \le \eta < \infty$, where η_L is the lower constant limit at which relation (10) is satisfied.

From Eq. (10), we have

$$\dot{f}(0) = \frac{U_e}{U_o} = \frac{1}{\gamma} \tag{12}$$

The velocity ratio γ will be used in the following to normalize the momentum equation. From Eqs. (10) and (12), we can write

$$U = U_e(1 - \gamma\dot{f}) \tag{13}$$

$$\partial U/\partial x = U_e'(1 - \gamma\dot{f}) - U_e\gamma'\dot{f} + U_e\gamma(L_o'/L_o)\eta\ddot{f} \tag{14}$$

$$\partial U/\partial y = -U_e\gamma/L_o\ddot{f} \tag{15}$$

The dots on f denote differentiation with respect to η, whereas the primes on U_e, L_o, and γ denote differentiation with respect to x. From the continuity Eq. (8), the velocity component V can be written

as

$$V(x,\eta) = -L_o \int_0^\eta U' \,\mathrm{d}\eta = V(x,\eta_L) - L_o \int_{\eta_L}^\eta U' \,\mathrm{d}\eta$$

The term $V(x,\eta_L)$ expresses the fact that self-similarity of the velocity defect has not been assumed to exist in the wall region. In the limit $Re = U_e L_o/\nu \to \infty$, this term vanishes since $\eta_L \to 0$, that is, the outer region becomes infinitely large with respect to the inner region. At finite Reynolds number, if the analysis was carried through with the above expression for V, one would find that self-similarity can only exist if $V(x,\eta_L)$ is a constant. This leads to the important conclusion that, at finite Reynolds number, the type of self-similarity considered here can only be obtained if the velocity defect profile is self-similar everywhere, that is, even in the inner region. Consequently, Eqs. (10) and (13–15) are also valid in the wall region. The integration of U' as given by Eq. (14) can therefore start at the wall, which gives

$$V = -L_o U'_e(\eta - \gamma f) + L_o U_e \gamma' f - L'_o U_e \gamma(\eta \dot{f} - f) \tag{16}$$

where the stream function f was defined such that $f(0) = 0$.

With the above equations, the mean momentum Eq. (9) becomes after simplification

$$\Lambda[2\dot{f} - \eta\ddot{f} + \gamma(f\ddot{f} - \dot{f}^2)] + \frac{L_o}{L'_o}\frac{\gamma'}{\gamma}(-\dot{f} + \gamma\dot{f}^2 - \gamma f\ddot{f}) + (\eta\ddot{f} - \gamma f\ddot{f})$$
$$= \frac{1}{\gamma}\left[\frac{\sigma_{12}}{L'_o}\dot{g}_{12} + \sigma_{11}\eta\dot{g}_{11} - \sigma_{22}\eta\dot{g}_{22}\right] \tag{17}$$

For complete self-similarity, and equivalently for equilibrium flow with the assumed type of similarity, the x-dependent coefficients in Eq. (17) must be constant. We therefore obtain the following necessary conditions:

$$\gamma = \frac{U_o}{U_e} = \text{const} \tag{18}$$

$$\frac{\sigma_{12}}{L'_o} = \frac{1}{L'_o}\frac{R_{12}}{U_e^2} = \text{const} \tag{19}$$

$$\sigma_{11} = \frac{R_{11}}{U_e^2} = \text{const} \tag{20}$$

$$\sigma_{22} = \frac{R_{22}}{U_e^2} = \text{const} \tag{21}$$

$$\Lambda = -\frac{L_o}{L'_o}\frac{U'_e}{U_e} = \text{const} \tag{22}$$

These similarity conditions are identical to CG's conditions, Eqs. (3–7), if L_o is replaced by δ. Condition (22) implies that a power law relation should exist between the freestream velocity and the length scale:

$$U_e \propto L_o^{-\Lambda} \tag{23}$$

Equations (18–21) are conditions imposed on the outer scales U_o, R_{12}, R_{11}, and R_{22} to achieve self-similarity. For instance, Eq. (18) states that the ratio of the outer velocity scale and the freestream velocity has to remain constant. Because of Eq. (12), it furthermore implies that the velocity defect profile is also self-similar at the wall. Note that it was already concluded when obtaining Eq. (16) that the velocity defect profile in the whole inner region has to be self-similar for finite Reynolds number TBL. As it will be seen now, the interpretation of these conditions depends, however, on what one believes is the asymptotic behavior of the TBL.

B. Theory of Castillo and George

Although they are cast in a different form, Eqs. (17–22) are identical to the similarity equation and conditions obtained by CG if L_o is replaced by δ. CG assumed that the ratios in Eqs. (18–21) are constants different than zero in the limit of an infinite Reynolds number. In other words, for them the velocity defect and Reynolds stresses do not vanish in that limit. They further assumed that Eqs. (18–21) are outer scale definitions rather than conditions for self-similarity. They therefore considered that the outer scales for the velocity defect, Reynolds normal stresses, and Reynolds shear stress are, respectively, U_e, U_e^2, and $U_e^2\,\mathrm{d}\delta/\mathrm{d}x$. As it will be seen in the next subsection, the commonly accepted view of the asymptotic behavior of TBL (and turbulent flows in general) is, however, different. In the classical treatment [3], it is rather assumed that velocity defect and Reynolds stresses vanish in the limit of an infinite Reynolds number. Consequently, U_e, U_e^2, and $U_e^2\,\mathrm{d}\delta/\mathrm{d}x$ cannot be the outer scales for the velocity defect and the Reynolds stresses in the classical viewpoint.

As mentioned in the Introduction, CG showed by analyzing several databases that TBLs appear to be characterized by only three possible values of Λ within experimental uncertainty (0.22 for APG, 0 for ZPG, and -1.92 for FPG). They concluded from this observation that almost all PG TBL, including very strong APG cases, appear to be equilibrium boundary layers since Eq. (22) is satisfied. They argued that the fact that U_e did not scale the velocity defect of most TBLs (i.e., condition (18) was not satisfied, they did not check the other even more demanding conditions (19–21) for the Reynolds stress scales) is not a problem because their analysis is only strictly valid at an infinite Reynolds number. For them, the mean velocity defect profiles of these TBLs can show dependence on Reynolds number and upstream conditions when scaled with U_e without invalidating their conclusion about flow equilibrium.

But mathematically, Eq. (17) gives no room for interpretation. Self-similarity of type (10) and (11), and hence equilibrium corresponding to it, can exist only if conditions (18–22) are all satisfied, whatever the Reynolds number. If on the other hand it is considered that the analysis is only strictly valid at an infinite Reynolds number, then it should not be invoked to determine if finite Reynolds number TBLs are in equilibrium. In this case, one would have to compute streamwise-mean-momentum balances from the experimental results to check if equilibrium exists. We have, however, shown that the similarity equations remain valid at finite Reynolds number (but only if the velocity defect is self-similar throughout the boundary layer).

CG further claimed that if Λ always takes the same value for a given sign of PG, then there exists a unique solution for the self-similar defect profile for all flows with the same sign of PG. Hence, the self-similar defect profile is independent of the pressure gradient strength and history. It only depends on the sign of the PG. To arrive at such a conclusion, one has to assume that the whole right-hand side of Eq. (17) is also independent of the pressure gradient strength and history. As we have seen in the previous section with Figs. 4 and 5, this is physically impossible. The Reynolds stress profiles are highly dependent on the pressure gradient strength and history (whatever the outer scales chosen). Most of the flows shown in Figs. 4 and 5 are not necessarily self-similar but there is no reason to believe that self-similar TBLs should behave differently. Moreover, even if one assumes like CG that the scale ratios γ, σ_{12}, σ_{11}, and σ_{22} do not vanish in the limit of an infinite Reynolds number, it cannot be concluded from the theory that they are independent of the pressure gradient strength and history in that limit, that is, always take the same value for a given sign of PG.

To summarize, in the context of the above general similarity theory:

1) Self-similarity and hence equilibrium of the corresponding type is only possible if all of the conditions (18–22) are satisfied. Conditions (18–21) imply that for a given flow, the profiles of velocity defect, Reynolds normal stresses, and Reynolds shear stress normalized, respectively, with U_e, U_e^2, and $U_e^2\,\mathrm{d}\delta/\mathrm{d}x$ should be self-similar. TBLs rarely behave in this manner. The only cases known to us are the traditional equilibrium boundary layers. This is expected since as it will be seen in Sec. III.D, the traditional equilibrium TBLs form a subcategory of the general self-similar TBLs considered up to now.

2) Even if one believes like CG that the scale ratios $\gamma, \sigma_{12}, \sigma_{11}$, and σ_{22} do not vanish in the limit of an infinite Reynolds number, nothing says that they should be independent of x for a given flow in that limit. Therefore, it cannot be concluded that most TBLs in the asymptotic limit are self-similar TBLs.

3) It also cannot be concluded that there exist only three self-similar velocity profiles (one each for ZPG, APG, and FPG boundary layers).

C. Generalized Traditional Theory

So far the general similarity theory has provided useful but rather limited information about self-similar TBLs. It will be seen now that physical arguments and the commonly accepted view of the asymptotic behavior of TBL will allow us to go one step further. To discuss the classic theory of turbulence as applied to TBLs, various flow scales need to be introduced. The length and time scales of the external flow are streamwise scales associated with the rate of change of U_e and they can be expressed as [28]

$$L_e = -\frac{U_e}{U_e'} \quad \text{and} \quad T_e = \frac{L_e}{U_e} = -\frac{1}{U_e'}$$

In the case of the ZPG TBL, $L_e \to \infty$ and we use instead the streamwise distance x from a properly defined origin. The outer length and time scales are, respectively, L_o and $T_o = L_o/U_o$. We can also define the inner length scale as L_i. In the case of TBLs with zero or mild PG, $L_i = \nu/u_\tau$.

The fundamental assumptions of the asymptotic theory of turbulence are [28]

$$\frac{L_o}{L_e} \to 0 \quad \text{and} \quad \frac{L_i}{L_o} \to 0 \quad \text{as } Re \to \infty$$

Furthermore, from physical and dimensional arguments, the outer time scale T_o, characteristic of turbulent transport, is assumed to be proportional to the streamwise time scale T_e for all Reynolds numbers. This implies that

$$\frac{U_o}{U_e} \propto \frac{L_o}{L_e} \quad \forall\ Re$$

Consequently, in the limit of an infinite Reynolds number,

$$\gamma = \frac{U_o}{U_e} \to 0 \quad \text{and} \quad \beta = \frac{T_o}{T_e} = -\frac{L_o}{U_o}U_e' = \frac{-L_o}{\gamma}\frac{U_e'}{U_e} \text{ remains finite}$$

Note that $\beta = 0$ only for the ZPG TBL. Vanishing γ means that U_e cannot be the outer velocity scale in the asymptotic limit. In the Introduction, it was discussed why U_e cannot be the outer velocity scale even at finite Reynolds number. Vanishing γ also means that the velocity defect vanishes in the outer region ($U \to U_e$) in the limit of an infinite Reynolds number; see Eq. (13). It basically says that in the asymptotic limit, turbulent transport becomes negligible with respect to mean momentum advection and pressure forces:

$$\frac{U_o^2/L_o}{U_e^2/L_e} = \left(\frac{U_o}{U_e}\right)\frac{L_e}{L_o} \propto \frac{U_o}{U_e} \to 0 \quad \text{as } Re \to \infty$$

The outer region essentially behaves as an inviscid flow zone. The same is not true of the inner region but it has become infinitely small with respect to the outer region. Hence in the limit $Re \to \infty$, the shape factor $H \to 1$ and the Reynolds stresses vanish with respect to U_e^2.

These asymptotic behaviors are not necessarily easy to conceptualize. For instance, the argumentation based on vanishing turbulence might seem to conflict with the theory of turbulence which itself is only strictly valid in the limit of an infinite Reynolds number but it does not. In a limit process, a physical mechanism can approach its asymptotic character while at the same time vanishing. For the same reason, the self-similar TBL is more rigorously defined in the limit of an infinite Reynolds number, with a single family of asymptotic solutions for $\dot{f}$, but at the same time its velocity defect and Reynolds stresses have become vanishingly small with respect to the external flow. In other words, from the perspective of the global flow, it is as if the TBL does not exist anymore.

In strong APG TBL, the velocity defect in the outer region is important at finite Reynolds number and can even be of the same order of magnitude as U_e. But even in these flows, the primary cause of velocity defect in the outer region is turbulent transport of momentum. Thus, if turbulent transport becomes negligible with respect to mean momentum advection and pressure forces, then the velocity defect in the outer region becomes infinitely small with respect to U_e. Hence even in strong APG flows, $H \to 1$ as $Re \to \infty$. Note that this does not mean that the velocity defect shape, the shape of $\dot{f}$, does not depend on the pressure gradient. It will be seen that it depends on β and that it can be characterized by the defect shape factor G presented below.

Returning to the similarity theory, by noting that $\Lambda = \beta\gamma/L_o'$ and that $\gamma' = 0$, the similarity Eq. (17) can be written as

$$\beta[2\dot{f} - \eta\ddot{f} + \gamma(f\ddot{f} - \dot{f}^2)] + \frac{L_o'}{\gamma}(\eta\ddot{f} - \gamma f\ddot{f}) = \frac{R_{12}}{U_o^2}\dot{g}_{12} + L_o'\left[\frac{R_{11}}{U_o^2}\eta\dot{g}_{11} - \frac{R_{22}}{U_o^2}\eta\dot{g}_{22}\right] \tag{24}$$

From a mathematical viewpoint, it can be seen from Eq. (24) that it is not required that β be a constant for self-similarity. However, it is reasonable to assume from a physical viewpoint that flow equilibrium necessarily implies a constant ratio of turbulent and streamwise time scales. With this assumption, the similarity conditions become

$$\beta = \frac{T_o}{T_e} = -\frac{L_o}{U_o}U_e' = \frac{-L_o}{\gamma}\frac{U_e'}{U_e} = \text{const} \tag{25}$$

$$\gamma = \frac{U_o}{U_e} = \text{const} \tag{26}$$

$$L_o' = \text{const} \tag{27}$$

$$\frac{R_{12}}{U_o^2} = \text{const} \tag{28}$$

$$\frac{R_{11}}{U_o^2} = \text{const} \tag{29}$$

$$\frac{R_{22}}{U_o^2} = \text{const} \tag{30}$$

β is the ratio of the turbulent time scale and the external flow time scale but it is also the term in the equation of motion (24) that expresses the role of the pressure gradient. It has therefore traditionally been defined as a pressure gradient parameter. As can be seen from Tables 1–3, whatever the choice of outer velocity scale U_o (u_τ and U_{ZS} in these cases) the similarity parameter β indeed reflects the local impact of the pressure gradient strength and history on the TBL. Therefore, if the assumption leading to condition (25) is accepted, then self-similar TBLs are necessarily a function of the pressure gradient strength and history. This is in agreement with the empirical evidence that was shown in the previous section.

Another useful pressure gradient parameter is

$$\Pi = \frac{\beta}{\gamma} = \frac{-L_o}{\gamma^2}\frac{U_e'}{U_e} = \frac{U_e^2/L_e}{U_o^2/L_o}$$

The parameter Π is basically the ratio of the pressure force scale and the Reynolds-stress-gradient scale. A constant value of Π represents therefore a constant ratio between the pressure and Reynolds stress gradients. This is expected because self-similarity necessarily implies equilibrium, that is, that the terms in the governing equations must maintain the same relative weight as the flow develops. Note,

Table 3 Self-similar stations and the corresponding similarity parameters

Experiment	Stations showing self-similarity with ZS	Self-similarity of Reynolds stresses	Λ	γ_{ZS}	β_{ZS}	G_{ZS}	Π_{ZS}
SJ	3 to 10 out of 12	No	0.22	0.17–0.20	0.01–0.066	1.63–1.54	0.043–0.254
MP30	Last 2 out of 6	No	0.33	0.23–0.25	0.061–0.067	1.52–1.49	0.266
MP10	Last 2 out of 6	No	0.30	0.26–0.29	0.055–0.061	1.50–1.49	0.212
SK	All 7 stations	Yes	0.22	0.36–0.35	0.046–0.047	1.41–1.42	0.129–0.136
P	Last 3 out of 10	No data	0.16	0.36–0.41	0.049–0.052	1.42–1.39	0.145–0.120
DF2	7 to 11 out of 12	?	0.19	0.42–0.50	0.035–0.041	1.31–1.21	0.097–0.070
DF1	7 to 11 out of 12	?	0.20	0.43–0.53	0.036–0.043	1.31–1.20	0.090–0.072
DF3	7 to 11 out of 12	?	0.17	0.47–0.56	0.031–0.042	1.28–1.21	0.077–0.057
MRL	4 and 5 out of 6	Yes	0.18	0.50–0.54	0.021–0.023	1.36–1.37	0.047–0.038

however, that Π has the disadvantage of becoming single valued (infinite) when $Re \to \infty$.

Like for Π, the condition $\Lambda = \text{const}$ does not appear explicitly in the above conditions but it is hidden in conditions (25–27). As mentioned in the Introduction, CG, Castillo et al. [15] and Castillo and Wang [16] have shown that most TBLs appear to be characterized by only three possible values of Λ within experimental uncertainty (0.22 for APG, 0 for ZPG, and -1.92 for FPG). They also found that even in flows with rapid changes of pressure gradient, TBLs seem to go rapidly from one constant value of Λ (the FPG, ZPG, or APG one) to another. The similarity parameter Λ is therefore not a pressure gradient parameter in the sense that it does not reflect the dynamic role of the pressure gradient in the momentum equation. Physically, the parameter Λ rather expresses the fact that the boundary layer growth rate is directly proportional to the ratio of the outer and streamwise length scales:

$$\frac{\mathrm{d}L_o}{\mathrm{d}x} = \frac{1}{\Lambda}\frac{L_o}{L_e} \tag{31}$$

Because conditions (25) and (26) imply a constant length scale ratio L_o/L_e, condition (27) goes one step further than Eq. (31) and states that the outer length scale has to vary linearly with streamwise distance

$$L_o = \frac{\beta\gamma}{\Lambda}(x - x_o) \tag{32}$$

where x_o is the virtual origin of the equilibrium state (where $L_o = 0$). L_o can of course increase ($x > x_o$), decrease ($x < x_o$), or remain constant depending on the PG conditions. Note that decreasing L_o occurring in very strong FPG conditions implies $\Lambda > 0$, which puts some doubt on the uniqueness of the three values of Λ suggested by CG (0.22 for APG, 0 for ZPG, and -1.92 for FPG with $L_o = \delta$). Recall that the values of Λ when $L_o = \delta$ were found to be similar but not identical (0.16–0.33) for the nine APG flows presented in the previous section. Schofield [29] reported values of Λ between 0.21 and 0.26 for 12 different traditional equilibrium boundary layers in APG conditions.

Relation (32) together with condition (23) indicates that a power law relation between U_e and x is necessary:

$$U_e \propto L_o^{-\Lambda} \propto (x - x_o)^{-\Lambda} \tag{33}$$

In the case of the traditional equilibrium boundary layers, such conditions on the flow development have been confirmed experimentally. For instance, SK obtained $\Lambda = 0.22$ and a linear growth with streamwise distance of δ, δ^*, and θ. In the case of two APG TBL maintained on the verge of separation (two different inflow conditions), Elsberry et al. [23] also found linear growth of the length scales and $\Lambda = 0.18$ and 0.21. Note that self-similarity was found with different velocity scales for velocity defect and the Reynolds stresses for these two flows (but ZS scaling was not tested).

Important information can also be obtained from the following parameters used in the classical similarity theory (here written in general terms with L_o and U_o):

$$F_1 = \int_0^\infty \frac{U_e - U}{U_o}\,\mathrm{d}\eta = \frac{1}{\gamma}\frac{\delta*}{L_o} \tag{34}$$

$$F_2 = \int_0^\infty \left(\frac{U_e - U}{U_o}\right)^2 \mathrm{d}\eta = \frac{1}{\gamma}\left(F_1 - \frac{1}{\gamma}\frac{\theta}{L_o}\right) \tag{35}$$

$$G = \frac{F_2}{F_1} = \frac{1}{\gamma}\left[1 - \frac{1}{H}\right] \tag{36}$$

G is the general form of the defect shape factor initially introduced by Clauser [4] with the scales u_τ and Δ. Because the velocity defect profiles are self-similar throughout the boundary layer at finite Reynolds number, that is, even in the inner region, and because $\gamma = \text{const}$, the following relations are obtained in the case of self-similar TBLs:

$$F_1 = \text{const} \Rightarrow \frac{\delta^*}{L_o} = \text{const} \qquad F_2 = \text{const} \Rightarrow \frac{\theta}{L_o} = \text{const}$$

$$G = \text{const} \Rightarrow H = \text{const}$$

Thus like it was found for the length scale L_o (which can be taken to be δ or Δ), the displacement thickness δ^* and the momentum thickness θ also grow linearly with streamwise distance and both shape factors are constant. For traditional equilibrium boundary layers, these behaviors of the boundary layer parameters are confirmed experimentally by SK. They will be checked in the next section for the flow cases studied here. However, Table 2 already shows that H is not constant for all the flows except SK because of a lack of self-similarity near the wall.

We will now consider self-similarity and equilibrium in the limit of an infinite Reynolds number. In that limit, $\gamma \to 0$ and $L_o' \to 0$. It can be further assumed that the scale ratios in Eqs. (28–30) have to remain finite and different than zero. The similarity Eq. (24) therefore becomes in the limit of an infinite Reynolds number:

$$\beta(2\dot{f} - \eta\ddot{f}) + \frac{L_o'}{\gamma}\eta\ddot{f} = \frac{R_{12}}{U_o^2}\dot{g}_{12} \tag{37}$$

In the asymptotic limit, the similarity conditions are therefore

$$\beta = \text{const} \tag{38}$$

$$\frac{\gamma}{L_o'} = \text{const} \tag{39}$$

$$\frac{R_{12}}{U_o^2} = \text{const} \tag{40}$$

As a final remark, note that if the assumptions stated in this subsection are accepted, then we have just shown that most of the results of the traditional similarity theory [4–8] remain valid even if the outer scales are left unspecified and are expressed in their most general form. The above is therefore a generalized form of the traditional similarity theory.

D. Theory with Common Velocity Scale

The studies about scaling of the TBL discussed in the Introduction and the experimental results presented in the previous section strongly suggest that U_{ZS} is a proper outer velocity scale for the velocity defect as well as for all the Reynolds stresses. In fact for TBL in general (APG, FPG, ZPG, complex PG, rough wall, ...), a better choice than common ZS scaling for the mean velocity defect and the Reynolds stresses does not seem to exist. In many TBL, the Reynolds stresses do not scale with the various scales proposed for ZPG TBL (u_τ^2, U_e^2, or $u_\tau U_e$) although they do with U_{ZS}^2. We will therefore adopt common outer scaling with the scales U_{ZS} and δ.

By assuming a common outer velocity scale for the velocity defect and the Reynolds stresses, that is, $R_{ij} = U_o^2$ for all values of i and j, the six similarity conditions (25–30) reduce to the first three conditions (25–27). If we replace the outer velocity and length scales U_o and L_o by the skin friction velocity u_τ and the Rotta–Clauser length scale Δ in Eqs. (25–27), we obtain the necessary conditions of the traditional similarity theory. If instead we replace them by U_{ZS} and δ, we get the desired new set of necessary conditions for self-similarity with the ZS scales:

$$\beta_{ZS} = \frac{-\delta}{U_{ZS}} U_e' = \frac{-\delta}{\gamma_{ZS}} \frac{U_e'}{U_e} = \text{const} \tag{41}$$

$$\gamma_{ZS} = \frac{U_{ZS}}{U_e} = \frac{\delta^*}{\delta} = \text{const} \tag{42}$$

$$\delta' = \text{const} \quad \text{or} \quad \Lambda = -\frac{\delta}{\delta'} \frac{U_e'}{U_e} = \text{const} \tag{43}$$

At this point, we can ask ourselves if δ is the appropriate length scale to use in combination with U_{ZS}. Following the argument of Rotta [6], because we are considering the outer region, we can try to define a length scale based solely on the velocity defect profile. By defining a thickness equivalent to the Rotta–Clauser thickness, we get

$$\Delta_{ZS} = \int_o^\infty \frac{U_e - U}{U_{ZS}} \, \mathrm{d}y = \frac{U_e}{U_{ZS}} \delta^* = \delta \tag{44}$$

Hence δ definitely seems to be the appropriate length scale to use in combination with U_{ZS}. From Eq. (44), we can see also that the area under the curve of the velocity defect plots scaled with ZS is necessarily one. Therefore, the defect profiles of two totally different flows can only differ by their shape when plotted with the ZS scaling, which implies that they can easily exhibit an apparent similarity.

IV. Results and Discussion

The various flows considered in Sec. II are now analyzed in the context of the present similarity analysis. As mentioned at the beginning of this paper, it is important to keep in mind that a flow (or flow region) can be in equilibrium even if a particular similarity theory would define it as a "nonequilibrium" flow. Conversely, if a flow is found to be in equilibrium according to a given similarity analysis, then it is in equilibrium regardless of the similarity assumptions. It will, however, be assumed that similarity conditions (25–30) define the most general type of self-similarity for TBLs. Hence, these conditions have to be satisfied for a TBL to be in equilibrium. The particular class of equilibrium TBL that satisfies the similarity conditions with ZS scaling, conditions (41–43), will be referred to as ZS-type equilibrium TBL.

We will first verify if the linear growth with streamwise distance of δ, δ^*, and θ exists. Figure 6 shows the streamwise evolutions of δ, δ^*, and θ for six flow cases. The results for flows MP30, DF1, and DF3 are not shown but they are very similar to those of their companion flow cases, MP10 and DF2, respectively. The streamwise extent of the measurement zones shown is expressed on each plot in terms of δ_{av}, the average boundary layer thickness between the first and the last measurement stations. Not enough data points are available in the zones of self-similar defect profiles of flows MP10, P, and MRL to determine if those zones correspond to linear growth of the length scales. Linear growth is definitely not present in the self-similar defect profile zone of flow SJ. Although the mean velocity defect profiles were self-similar with ZS scaling, the SJ flow is not an equilibrium flow. This will be further supported by the behavior of the similarity parameters β_{ZS} and γ_{ZS}. The SK and DF flows do show a linear streamwise evolution of all length scales in the self-similar defect profile zones. The length scales should, however, all have the same virtual origin of the equilibrium state, x_o. This is confirmed for the SK flow but not for the other flows.

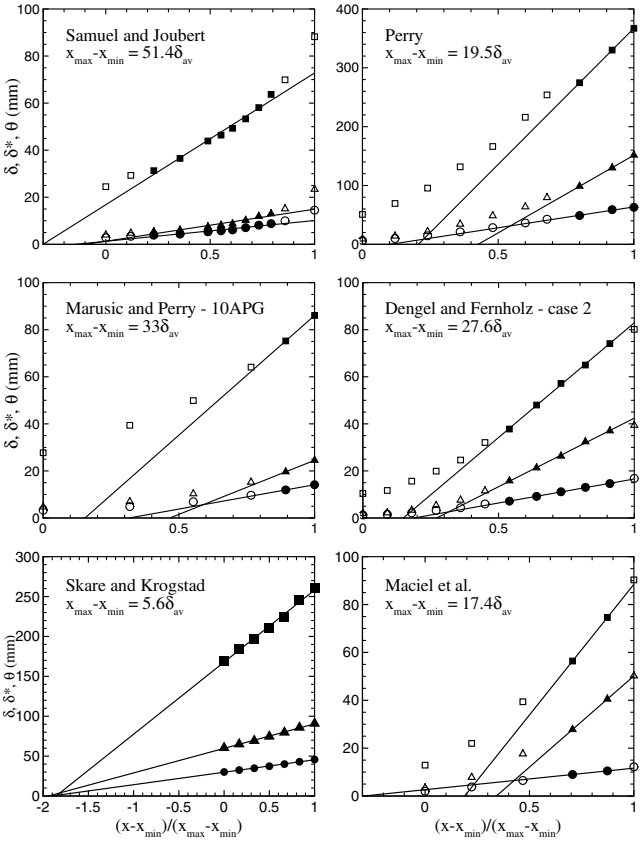

Fig. 6 Streamwise evolution of δ_{99} (open squares), δ^* (open triangles), and θ (open circles). Filled symbols correspond to the positions of self-similar defect profiles. The lines are linear fits of the data in the self-similar regions. For each flow case, δ_{av} is the average boundary layer thickness between x_{min} and x_{max}.

We will now determine if there is a power law relation between U_e and δ by analyzing the behavior of the similarity parameter Λ; see Eq. (23). To do so, we adopt the strategy of CG which consists in plotting U_e vs δ in a log-log scale and calculating Λ when it becomes constant through linear regression. In this manner, the uncertainty associated with calculating the derivatives $\mathrm{d}\delta/\mathrm{d}x$ and $\mathrm{d}U_e/\mathrm{d}x$ is removed. It does not permit, however, to determine local values of Λ but its evolution can be followed qualitatively. Two illustrative examples are presented in Fig. 7 with the data of DF2 and MRL. For flow case DF2, the boundary layer definitely seems to reach a constant value of Λ in the self-similar region. A linear regression of the five points in this region gives a value of Λ of 0.19, which is close to the range of values found by CG, Castillo et al. [15], and Castillo and Wang [16] (0.21–0.25).

Because the DF2 TBL started as an FPG boundary layer and therefore with a negative Λ, it is interesting to note the overshoot of Λ (>0.19) at the first stations. A similar behavior is found with the MRL flow. It is probably linked to the fairly rapid changes of PG conditions in these flows. In the case of the MRL flow, although more data points would be necessary for a firm conclusion, the condition $\Lambda = \text{const}$ seems to be reached before self-similarity of the profiles occurs. A similar trend has also been found with the MP flows. Of course, in the case of the MRL flow, one could always argue that the

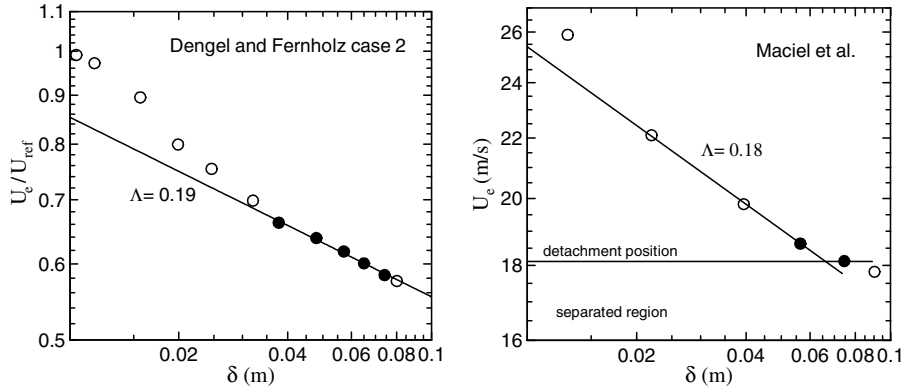

Fig. 7 Log-log plot of U_e vs δ for flows DF2 and MRL, along with fits of Eq. (23). Filled symbols correspond to the positions of self-similar defect profiles.

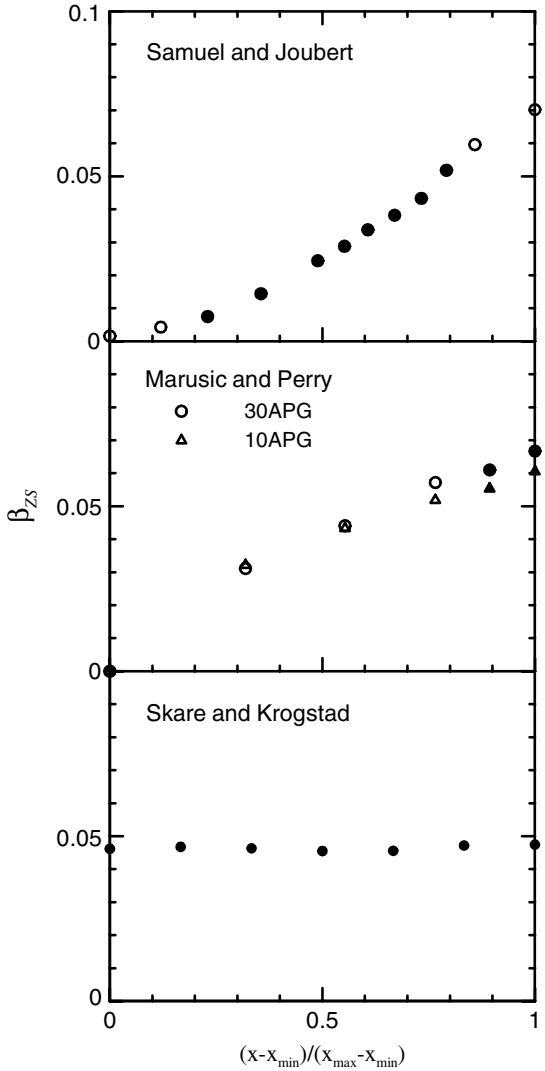

Fig. 8 Streamwise evolution of β_{ZS} for the milder APG flows. Filled symbols correspond to the positions of self-similar defect profiles.

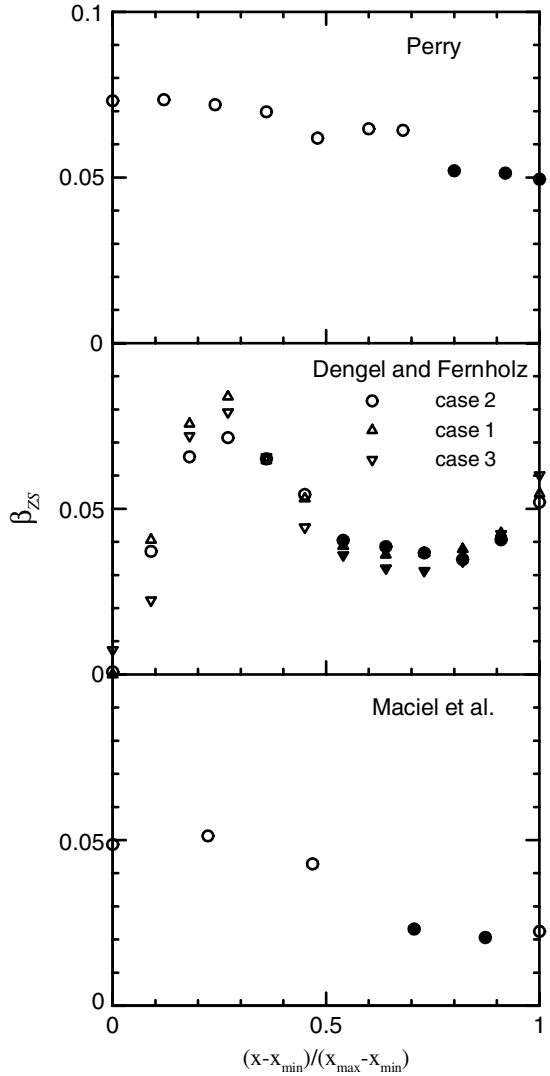

Fig. 9 Streamwise evolution of β_{ZS} for the stronger APG flows. Filled symbols correspond to the positions of self-similar defect profiles.

slope corresponding to the last 3 data points is the one that gives the value of Λ for the self-similar state, $\Lambda = 0.09$ in this case. But because the last data point is in the separated flow zone, we have assumed that the change of slope corresponds to the departure from the self-similar state due to separation. The condition $\Lambda = \text{const}$ is a necessary condition for self-similarity but, in practice, it is probably not a very sensitive way of verifying it.

The streamwise evolutions of the similarity parameters β_{ZS} and γ_{ZS} and of the pressure gradient parameter Π_{ZS} are shown in Figs. 8–13. From Figs. 8 and 9, it is seen that the zones where the velocity defect profiles are self-similar (filled symbols) correspond generally to a relatively constant value of the similarity parameter β_{ZS}. The exception is the SJ flow case where β_{ZS} keeps steadily increasing even in the large zone of self-similarity of the defect profiles. This result can be put in parallel with the nonlinear streamwise evolution of the length scales previously discussed. Although the mean velocity defect profiles were self-similar with ZS scaling, the SJ flow is not an equilibrium flow of the type given by the present similarity analysis.

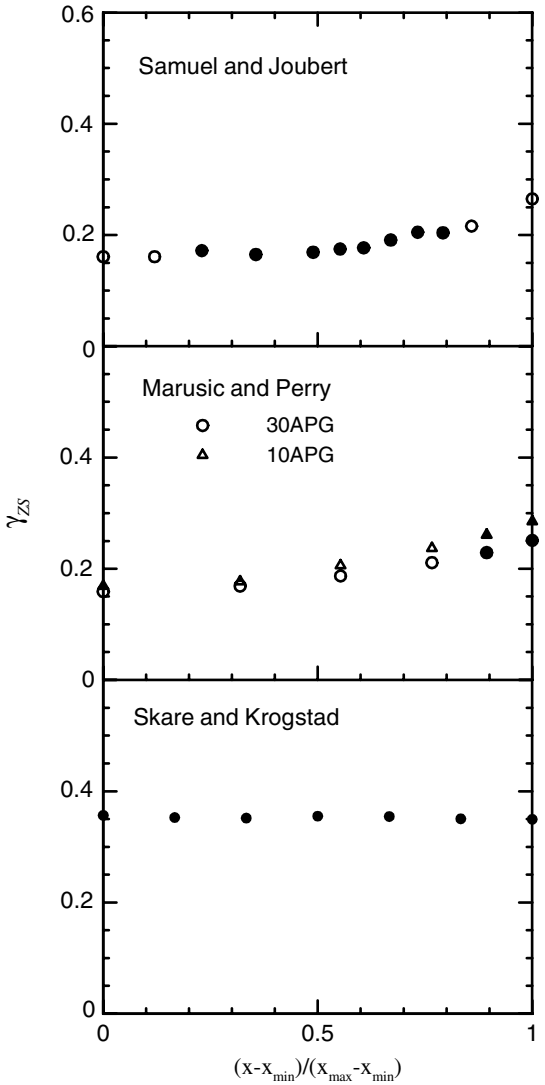

Fig. 10 Streamwise evolution of γ_{ZS} for the milder APG flows. Filled symbols correspond to the positions of self-similar defect profiles.

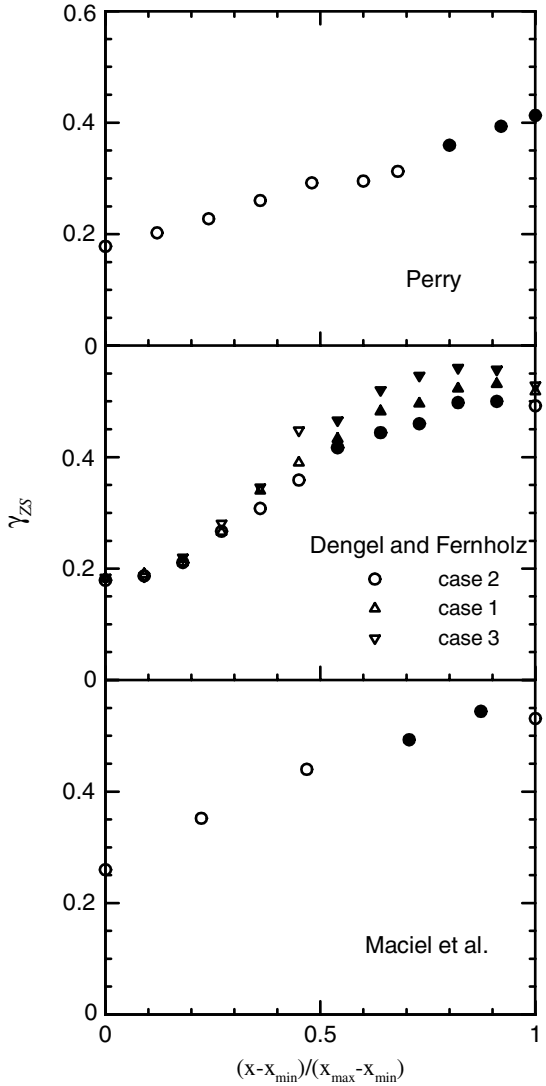

Fig. 11 Streamwise evolution of γ_{ZS} for the stronger APG flows. Filled symbols correspond to the positions of self-similar defect profiles.

Figures 10 and 11 show that in the zones of profile self-similarity, the similarity parameter γ_{ZS} does not become constant for the MP and P flows. It is constant for the SK flow and relatively so for the DF and MRL flows. Only the SK traditional equilibrium TBL can be considered to show a true constancy of all the similarity parameters (Λ, β_{ZS}, and γ_{ZS}). Slight evolutions are seen in the self-similarity zones of all the other flow cases. The flow cases of DF and MRL are particularly instructive. The self-similar zones of these flows correspond to a local minimum of β_{ZS} and a local maximum of γ_{ZS}. The similarity zone is in fact a transition zone from one behavior to another. These flows cannot therefore be considered to be in ZS equilibrium. In the framework of the present analysis, they are only in a state of near ZS equilibrium.

To verify and to better understand the equilibrium conditions of their flow, MRL have computed the streamwise-mean-momentum balance at all their measurement stations. Recall that flow equilibrium means that the terms in the governing equations must maintain the same relative weight as the flow develops. MRL found that this was almost achieved but not completely for the two stations where self-similarity exists. In particular, the results indicated that the pressure gradient term was still losing importance compared to all the other terms as the flow evolved. The streamwise evolution of the pressure gradient parameter Π_{ZS} (ratio of the pressure force scale and the Reynolds-stress-gradient scale) shown in Fig. 13 is in agreement with this observation since it decreases slightly in the self-similar zone. The momentum balance therefore indicates that the state of near ZS equilibrium of the MRL flow is in fact a true state of near equilibrium, that is, independent of any similarity assumption.

From Figs. 12 and 13, it is interesting to note that Π_{ZS} decreases as the severity of the APG environment increases. It is particularly small in the near-equilibrium zones of the very strong APG flows (DF and MRL). This is to be expected since the turbulent activity increases sharply as separation is approached. Note that Clauser's pressure gradient parameter β_T would not follow the same trend in these cases. It would rather tend to infinity. The evolution of Π_{ZS} is very different from one flow case to another.

The pressure gradient parameters Π_{ZS} and β_{ZS} are definitely more apt than β_T to characterize TBL in general PG conditions. The reason lies essentially in the fact that U_{ZS} is a turbulent velocity scale for general PG TBL whereas u_τ is not. Hence, Π_{ZS} and β_{ZS} truly reflect the local impact of the pressure gradient on the TBL for all flow conditions, even in strong adverse-pressure-gradient conditions and close to separation.

Table 3 summarizes the values of the similarity parameters in the self-similar zones of each flow. As expected, the defect shape factor G_{ZS} is seen to remain fairly constant or vary only slightly in the self-similarity zones of the flows considered. The shape factor H (Table 2) varies more importantly in all cases, except for the SK flow. From Eq. (36) it is seen that a variation of H while G_{ZS} remains constant can only be caused by a variation of γ_{ZS}. Thus because $1/\gamma_{ZS}$ is the value of the scaled velocity defect profile at the wall, Eq. (12), the variations of H reflect streamwise changes of the velocity defect profiles in the near wall zone.

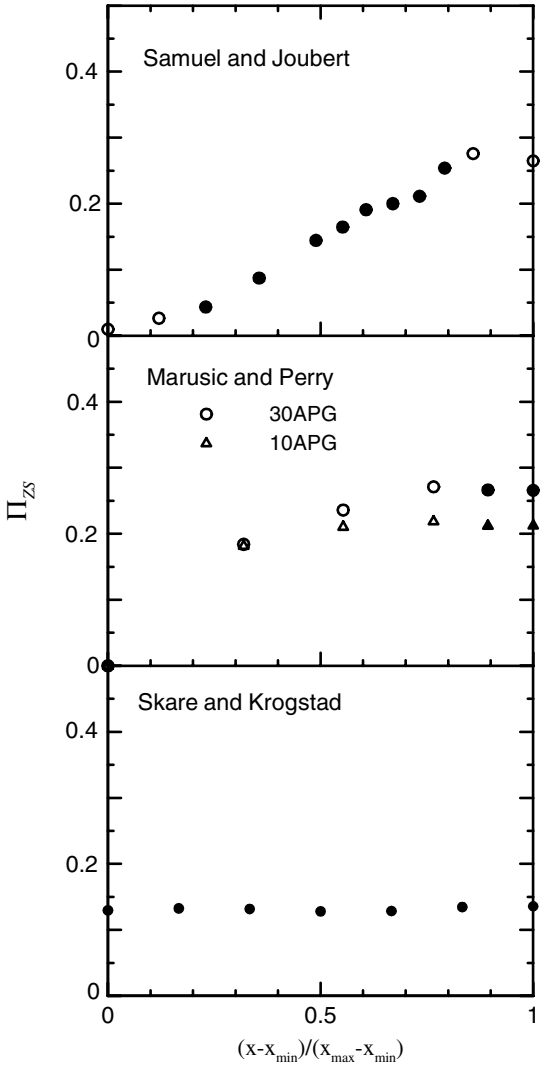

Fig. 12 Streamwise evolution of Π_{ZS} for the milder APG flows. Filled symbols correspond to the positions of self-similar defect profiles.

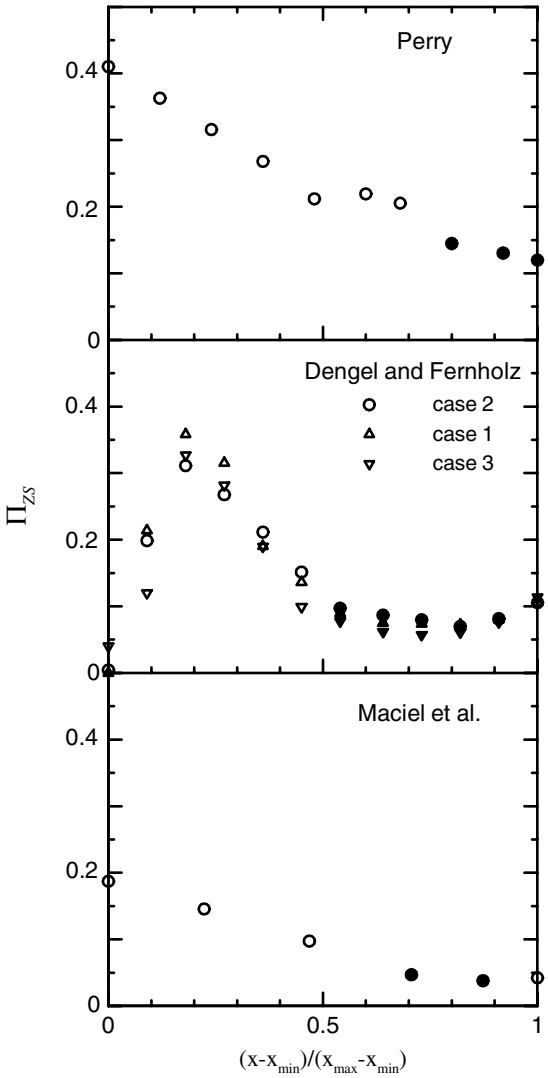

Fig. 13 Streamwise evolution of Π_{ZS} for the stronger APG flows. Filled symbols correspond to the positions of self-similar defect profiles.

The evolutions of the defect shape factor G_{ZS} with respect to γ_{ZS} and Π_{ZS} are shown, respectively, in Figs. 14 and 15. Because the shapes of the various self-similar defect profiles are close to one another, the defect shape factor G_{ZS} does not vary significantly. The dependence of G_{ZS} on the flow conditions is, however, clearly revealed by these figures. The data of DF and MRL do not follow the same trend. The fact that the DF flows are not planar flows but axisymmetric ones could play a role. The analysis of more databases will be pursued to help clarify this matter, among others.

V. Conclusions

This work is an attempt to put into perspective the impact of recent findings related to the subject of equilibrium boundary layers. Only APG TBL databases have been considered here although the analytical tools used are not restricted to that flow category. The similarity analysis of the outer region of TBL was first presented in a general form that encompasses all of the various similarity analyses found in the literature. Contrary to the interpretation of Castillo and George [13], it was shown that it cannot be concluded from the general similarity theory that most TBLs are in equilibrium and that there can only be three possible limiting velocity defect profiles (one each for ZPG, APG, and FPG). Two divergent viewpoints of the general similarity theory were discussed. Empirical and theoretical arguments were presented to support the viewpoint based on the classical treatment of turbulence. In that context, it was shown that the following fundamental results of the traditional similarity theory remain valid even if the outer scales are left unspecified and even if it is not assumed that the mean velocity defect and the Reynolds stresses share a common velocity scale:

1) The self-similar defect profile is a function of a pressure gradient parameter β that reflects the local impact of the pressure gradient strength and history.

2) Self-similarity implies a linear growth with streamwise distance of δ, δ^*, and θ and a power law relation between U_e and x.

3) TBLs found in the real world are almost never in a state of equilibrium, although they tend to approach it in some cases.

The traditional similarity theory is a valid theory but it cannot be used for TBLs in general. It forms a subset of the general similarity theory presented here that is only valid for TBLs in mild PG for which u_τ is a suitable turbulent velocity scale.

For TBLs in general (APG, FPG, ZPG, complex PG, rough wall, ...), a better choice than common ZS scaling for the mean velocity defect and the Reynolds stresses does not seem to exist for the moment. In many TBLs, the Reynolds stresses do not scale with the various scales proposed for ZPG TBL (u_τ^2, U_e^2, or $u_\tau U_e$) although they always do with U_{ZS}^2. Furthermore, as Castillo and George [13] and Castillo and Wang [16] have already found, the extent of self-similarity of the velocity defect profiles revealed by this scale is impressive. All the flows studied here exhibit self-similarity in localized but significant flow regions. The same is, however, not true of the Reynolds stress profiles. Astonishingly, with the exception of the SK flow, the flow that deviates the most from the traditional definition of an equilibrium boundary layer

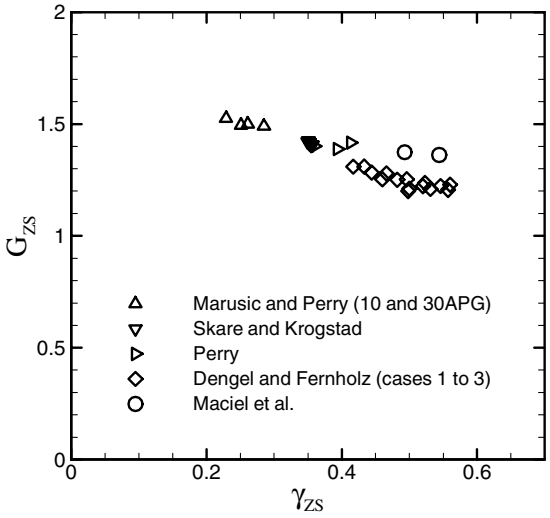

Fig. 14 Defect shape factor G_{ZS} against γ_{ZS}. Only date in self-similarity zones.

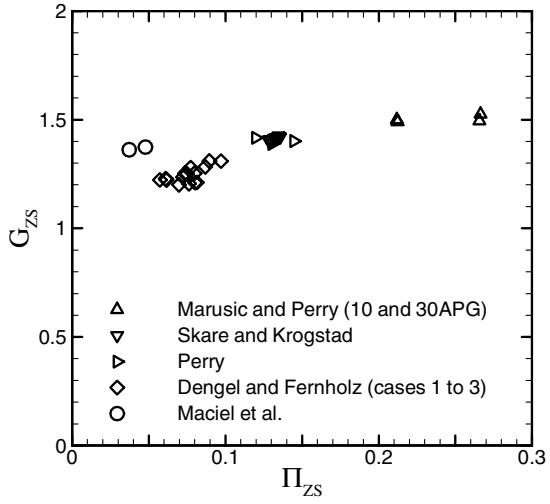

Fig. 15 Defect shape factor G_{ZS} against Π_{ZS}. Only date in self-similarity zones.

(the one with the largest variations of C_f and β_T) is the one where self-similarity of the Reynolds stress profiles was also found. The explanation seems to lie at least partly in the fact that in strong APG conditions, the outer region of the boundary layer essentially behaves as an inertial flow zone where equilibrium is more likely to be nearly achieved.

The study of the similarity parameters revealed even more sharply the conclusions that were drawn from inspection of the velocity defect and Reynolds stress profiles. It confirmed that only the SK flow can be said to be in equilibrium (or extremely close to it) despite the very good collapse of the velocity defect profiles in significant regions of all the flows studied here. In the region of self-similar defect profiles, the SJ flow is clearly not in ZS equilibrium (the class of flow equilibrium corresponding to complete self-similarity with the ZS scaling) whereas all the others are only in a state of near ZS equilibrium.

In the case of the MRL flow, MRL have confirmed by direct inspection of the streamwise evolution of the terms in the mean momentum equation that their flow does not achieve complete equilibrium although it is very close to it. Such a conclusion might appear to be in contradiction with the fact that the MRL profiles seem to reveal complete self-similarity but it is not. In the framework of the present similarity theory, equilibrium at finite Reynolds number is only possible if the velocity defect profile is self-similar throughout the boundary layer. However impressive the collapse of the MRL velocity defect profiles might be, the profiles are not self-similar near the wall and at the wall (γ_{ZS} varies). Hence, the MRL flow does not in fact achieve the required complete self-similarity although it is very close to it.

We should add that, except for the SK flow, self-similarity of the velocity defect, Reynolds normal stress, and Reynolds shear stress profiles is not obtained when scaling them, respectively, with U_e, U_e^2, and $U_e^2\,\mathrm{d}\delta/\mathrm{d}x$ (results not presented). This means that none of the conditions (18–21) of the general similarity analysis were satisfied for the flows studied here except for the SK flow. Thus complete self-similarity of the most general type given by Eqs. (10) and (11) simply does not exist for these flows regardless of the outer scales.

The general similarity theory presented here has provided a consistent theoretical framework to understand the surprising extent of self-similarity obtained with the ZS scaling. It has also led to a new pressure gradient parameter β_{ZS} which, as opposed to β_T, is able to characterize the local impact of the pressure gradient on the turbulent boundary layer in all flow conditions, even in strong APG conditions and close to separation.

Acknowledgments

Financial support from NSERC of Canada through its research grant programs is gratefully acknowledged by the authors. They also wish to thank the reviewer for his many pertinent comments and Philippe Bélanger-Vincent for his help in analyzing the data. Thanks are also due to Luciano Castillo and Brian Brzek for sharing their databases.

References

[1] Buschmann, M. H., and Gad-el-Hak, M., "Debate Concerning the Mean Velocity Profile of a Turbulent Boundary Layer," *AIAA Journal*, Vol. 41, No. 4, April 2003, pp. 1–8.

[2] George, W. K., "Recent Advancements Toward the Understanding of Turbulent Boundary Layers," AIAA Paper 2005-4669, June 2005.

[3] Panton, R. L., "Review of Wall Turbulence as Described by Composite Expansions," *Applied Mechanics Reviews*, Vol. 58, No. 1, 2005, pp. 1–36.

[4] Clauser, F. H., "The Turbulent Boundary Layer in Adverse Pressure Gradient," *Journal of Aeronautical Sciences*, Vol. 21, No. 2, 1954, pp. 91–108.

[5] Rotta, J., "Über die Theorie der turbulenten Grenzschichten," *Mitteilungen Max Planck Institut Strömungsforsch., Göttingen*, No. 1, 1950; translated as "On the Theory of Turbulent Boundary Layers," NACA TM-1344, 1953.

[6] Rotta, J. C., "Turbulent Boundary Layers in Incompressible Flow," *Progress in Aerospace Sciences*, Vol. 2, Nos. 1–2, 1962, pp. 1–219.

[7] Townsend, A. A., "*Structure of Turbulent Shear Flow*," 1st ed., Cambridge Univ. Press, New York, 1956.

[8] Townsend, A. A., "The Properties of Equilibrium Boundary Layers," *Journal of Fluid Mechanics*, Vol. 1, No. 6, 1956, pp. 561–73.

[9] Stratford, B. S., "An Experimental Flow with Zero Skin Friction Throughout its Region of Pressure Rise," *Journal of Fluid Mechanics*, Vol. 5, No. 1, 1959, pp. 143–155.

[10] Bradshaw, P., "The Turbulent Structure of Equilibrium Boundary Layers," *Journal of Fluid Mechanics*, Vol. 29, No. 4, 1967, pp. 625–645.

[11] East, L. F., and Sawyer, W. G., "An Investigation of the Structure of Equilibrium Turbulent Boundary Layers," *Turbulent Boundary Layers: Experiment, Theory and Modelling*, CP-271, AGARD, 1979, pp. 6.1–6.19.

[12] Skåre, P. E., and Krogstad, P. Å., "A Turbulent Equilibrium Boundary Layer near Separation," *Journal of Fluid Mechanics*, Vol. 272, 1994, pp. 319–348.

[13] Castillo, L., and George, W. K., "Similarity Analysis for Turbulent Boundary Layer with Pressure Gradient: Outer Flow," *AIAA Journal*, Vol. 39, No. 1, 2001, pp. 41–47.

[14] Zagarola, M. V., and Smits, A. J., "Mean-Flow Scaling of Turbulent Pipe Flow," *Journal of Fluid Mechanics*, Vol. 373, 1998, pp. 33–79.

[15] Castillo, L., Wang, X., and George, W. K., "Separation Criterion for Turbulent Boundary Layers via Similarity Analysis," *ASME Journal of Fluids Engineering*, Vol. 126, No. 3, May 2004, pp. 297–304.

[16] Castillo, L., and Wang, X., "Similarity Analysis for Nonequilibrium Turbulent Boundary Layers," *ASME Journal of Fluids Engineering*, Vol. 126, No. 5, Sept. 2004, pp. 827–834.

[17] Castillo, L., and Walker, D. J., "Effect of Upstream Conditions on the

Outer Flow of Turbulent Boundary Layers," *AIAA Journal*, Vol. 40, No. 7, 2002, pp. 1292–1299.

[18] Maciel, Y., Rossignol, K. S., and Lemay, J., "A Study of a Turbulent Boundary Layer in Stalled-Airfoil-Type Flow Conditions," *Experiments in Fluids*, published online 28 July 2006, DOI: 10.1007/s00348-006-0182-1, pp. 1–18.

[19] Buschmann, M. H., and Gad-el-Hak, M., "Structure of Turbulent Boundary Layers With Zero Pressure Gradient," AIAA Paper 2005-4813, June 2005.

[20] Mellor, G. L., and Gibson, D. M., "Equilibrium Turbulence Boundary Layers," *Journal of Fluid Mechanics*, Vol. 24, No. 2, 1966, pp. 225–253.

[21] Perry, A. E., and Schofield, W. H., "Mean Velocity and Shear Stress Distributions in Turbulent Boundary Layers," *Physics of Fluids*, Vol. 16, No. 12, Dec. 1973, pp. 2068–2074.

[22] Dengel, P., and Fernholz, H. H., "An Experimental Investigation of an Incompressible Turbulent Boundary Layer in the Vicinity of Separation," *Journal of Fluid Mechanics*, Vol. 212, 1990, pp. 615–636.

[23] Elsberry, K., Loeffler, J., Zhou, M. D., and Wygnanski, I., "An Experimental Study of a Boundary Layer that is Maintained on the Verge of Separation," *Journal of Fluid Mechanics*, Vol. 423, 2000, pp. 227–261.

[24] Angele, K., "Experimental Studies of Turbulent Boundary Layers Separation and Control," Ph.D. Thesis, Department of Mechanics, Royal Institute of Technology (KTH), Stockholm, Sweden, 2003, pp. 81–105.

[25] Samuel, A. E., and Joubert, P. N., "A Boundary Layer Developing in an Increasingly Adverse Pressure Gradient," *Journal of Fluid Mechanics*, Vol. 66, No. 3, 1974, pp. 481–505. Tabulated data known as "flow 141" from the 1980 AFOSR-IFP-Stanford Conference.

[26] Marusic, I., and Perry, A. E., "A Wall-Wake Model for the Turbulence Structure of Boundary Layers. Part 2. Further Experimental Support," *Journal of Fluid Mechanics*, Vol. 298, 1995, pp. 389–407.

[27] Perry, A. E., "Turbulent Boundary Layers in Decreasing Adverse Pressure Gradients," *Journal of Fluid Mechanics*, Vol. 26, No. 3, 1966, pp. 481–506.

[28] Tennekes, H., and Lumley, J. L., "*A First Course in Turbulence*," MIT Press, Cambridge, MA, 1972.

[29] Schofield, W. H., "Equilibrium Boundary Layers in Moderate to Strong Adverse Pressure Gradients," *Journal of Fluid Mechanics*, Vol. 113, 1981, pp. 91–122.

A. Tumin
Associate Editor